Arabian Journal of Chemistry (2023) **16**, 104800

King Saud University

Arabian Journal of Chemistry

www.ksu.edu.sa
www.sciencedirect.com

ORIGINAL ARTICLE

Biosynthesized gold nanoparticles using leaf extract of *Citrus medica* inhibit hepatocellular carcinoma through regulation of the Wnt/β-catenin signaling pathway

Bing Liu [a,1], Chenggang Li [a,1], Jun Han [a,1], Yongliang Chen [a,*], Zhiming Zhao [a,*], Hongwei Lu [b]

[a] *Faculty of Hepato-Pancreato-Biliary Surgery, The First Medical Center, Chinese PLA General Hospital, Beijing 100853, China*
[b] *Department of General Surgery, The Second Affiliated Hospital of Xi'an Jiaotong University, Xi'an, Shaanxi 710004, China*

Received 13 November 2021; accepted 9 March 2023
Available online 16 March 2023

KEYWORDS

Gold nanoparticles;
Leaf extract of *Citrus medica*;
Biosynthesis;
Characterization;
Hepatocellular carcinoma;
Wnt signaling pathway

Abstract Gold nanoparticle (AuNPs) influence the biomedical sciences owing to different potential characteristics and potential features. To date, the bioinspired fabrication of AuNPs is further recognized due to their safety and efficacy. In this study, we synthesized AuNPs using leaf extract of *Citrus medica* (*C. medica*) and well-characterized by dynamic light scattering (DLS), transmission electron microscopy (TEM), Fourier transform infrared spectroscopy (FTIR), X-ray diffraction (XRD), and UV–visible analyses. Afterward the selective anticancer effects of biosynthesized AuNPs against HepG2 cells were evaluated by different techniques including MTT, oxidative markers, qPCR, and western blot assays.

The results showed that the polyphenols of the *C. medica* leaf extract was responsible for the bioinspired reduction and stability of the AuNPs with a powder size in the range of 20–50 nm. Additionally, it was seen that biosynthesized AuNPs show selective inhibition on the proliferation of HepG2 (human liver cancer cell line) relative to THLE3 (normal adult liver epithelial cells) via generation of ROS and MDA, reduction of GSH level and SOD activity, and over expression of *Bax*/*Bcl-2* and *Caspase-3* mRNA. It was also shown that biosynthesized AuNPs regulate the Wnt signaling pathway through upregulation of phosphorylated GSK-3β known as the inactivated form of GSK-3β and downregulation of β-catenin and Cyclin-D1 at protein level. This study may hold great promise for development of NP-based anticancer agents, although it needs further investigations *in vivo*.

* Corresponding authors at: Faculty of Hepato-Pancreato-Biliary Surgery, The First Medical Center, Chinese PLA General Hospital, NO. 28, Fuxing Road, Beijing 100853, China. (Y. Chen, Z. Zhao).
E-mail address: chenyongl301@163.com (Y. Chen).
[1] Contributed equally to this study.

https://doi.org/10.1016/j.arabjc.2023.104800
1878-5352 © 2023 Published by Elsevier B.V. on behalf of King Saud University.

1. Introduction

With increasing awareness of green chemistry and biological processes, the use of environmentally friendly methods in the preparation of nontoxic nanomaterials seems necessary. Although various biological methods for bio-preparation of metal nanoparticles (NPs) are known, the use of organisms or other intermediates for the preparation of the NPs is expensive and limited. Therefore, the use of plants for the synthesis of NPs has received much attention due to the several advantages including feasible and cost-effective processes along with the utilization of nontoxic agents. In fact, plant-based biosynthesis of NPs can be considered as an environmentally friendly as well as economical and efficient approach (Elizabeth et al., 2022). Plant leaf extracts contain bioactive compounds, which act as potential reducing agents in the synthesis of different kinds of NPs (Elizabeth et al., 2022). Therefore, today, the use of plant extracts in the synthesis of metal NPs has received a great deal of attention in biomedical areas (Elizabeth et al., 2022).

In fact, several researches have been conducted on the use of plant extracts for the potential preparation of metal NPs with defined dimension and morphology (Vijayaraghavan and Ashokkumar, 2017).

Citrus medica (*C. medica*, Citron) is known as an underutilized fruit possessing different secondary metabolites (Chhikara et al., 2018). The major secondary metabolites present are reported to be limonene and its derivatives, citral, polyphenols, vitamin, nonana, etc., responsible for a number of therapeutic potentials (Chhikara et al., 2018). The different potential benefits of *C. medica* and its secondary metabolites in pharmacological studies are to trigger antioxidant (Chhikara et al., 2018; Taghvaeefard et al., 2021), antibacterial (Fratianni et al., 2019; Lou et al., 2017), anti-inflammatory (Mitropoulou et al., 2017) and hypoglycemic activities (Menichini et al., 2011). It has been also reported that *C. medica* extract has promising anticancer activities (Nair et al., 2018).

Therefore, *C. medica* extract has been introduced as a suitable, cost-effective and safe alternative in terms of green chemistry instead of using toxic and dangerous chemicals for the synthesis of different types of NPs including silver (Chandhirasekar et al., 2021), cobalt oxide (Siddique et al., 2021), and gold (Falahati et al., 2020).

One of the major problems in cancer treatment is that along with cancer cells, noncancerous cells are destroyed. In chemotherapy, the drug reaches the whole body while the target is only cancer cells. In radiation therapy, the location of the radiation can be more limited, but in any case, the radiation can damage some healthy cells. In surgery, sometimes removing the tumor requires sacrificing part of the healthy tissue around it, which the loss of the healthy tissues can lead to the loss of some functions. For this reason, in many cases, surgery is combined with chemotherapy or radiation therapy.

Gold is an element that rarely reacts chemically with other substances. For the same reason, it does not cause an allergic or immune reaction in the body.

Gold (Au) NPs are known as one the promising anticancer agent (Sharifi et al., 2019; Falahati et al., 2020). For example, it has been reviewed that AuNPs owing to plasmonic properties can be applied in the development of potential platforms in imaging, drug delivery, and therapy (Sharifi et al., 2019). Also, it has been reported that AuNPs can be used for the advancement of NPs-based thermal therapies (Devarakonda et al., 2017; 16. Kennedy et al., 2011).

Liver cancer has been proposed as a global health problem as the human hepatocellular carcinoma (HCC) is the fifth most common cause of cancer in the world and the third leading cause of death and morbidity in various types of cancer (McGlynn et al., 2021). Treatment of this complication with current approaches have many limitations in patients with metastatic tumors. Therefore, the development of more effective therapeutic platforms is important for improving the survival of patients and promising treatment of the disease in the advanced and recurrent stages of HCC.

Hepatocellular carcinoma HepG2 cells have shown a regulation in Wnt signaling pathways (Khalaf et al., 2018). In fact, the role of this important cellular pathway in the cell proliferation of different types of cancers has also been well demonstrated (Khalaf et al., 2018). In the Wnt signaling pathway, it activates catenin-β, which in turn results in the upregulation of Cyclin D1 mRNA/protein to direct the cell to invasion and proliferation (Khalaf et al., 2018).

Therefore, in this research, green method of AuNPs synthesis using *C. medica* leaf extract was introduced as an efficient way for the development of a nano-based anticancer platform against hepatocellular carcinoma HepG2 cell line through regulation of Wnt signaling pathway.

2. Materials and methods

2.1. Biosynthesis of AuNPs

For biosynthesis of AuNPs, 2 g of leaf extract of *C. medica* (collected from Southwestern China) after washing were cut into small pieces, added by 100 mL of double distilled water (DDW), boiled for 30 min with constant stirring, cooled down and filtered using Whatman filter paper (8 μm and 0.20 μm). The concentration of leaf extract of *C. medica* was calculated to be 22.35 mg/mL, assessed by a calibration curve. $HAuCl_4$ (Sigma-Aldrich 99% pure, Shanghai, China) with a concentration of 5 mM added into leaf extract of *C. medica* (2 mL) solution in a total volume of 8 mL with DDW. Then, the sample was mixed and constantly at room temperature, and the biosynthesis of the AuNPs was visually determined by the alteration in coloration of the solution. Afterwards, the sample was centrifuged (15,000 rpm for 50 min) folllowed by adding DDW to pellet, sonicating, repeating thrice, centrifugation, and drying the precipitate at 60–65 °C in a hot air oven. Finally, the AuNPs were used for further studies.

2.2. Total polyphenol assay

For total polyphenol assay, 25 μg/mL of leaf extract of *C. medica* either alone or with $HAuCl_4$ was added by Folin-Ciocalteu (0.25 N) and sodium carbonate (5%) and incubated for 50 min in the dark. Absorbance of the sample was read at 750 nm using a Perkin-Elmer Lambda 40 UV/Vis spectrometer. The data were then expressed as gallic acid equivalents (Conde-Hernández et al., 2014; de Camargo et al., 2014).

2.3. Characterization of AuNPs

A Perkin-Elmer Lambda 40 UV/Vis spectrometer was used to analyze the surface plasmon resonance of biosynthesized AuNPs. Zeta potential and diameter of biosynthesized AuNPs dissolved in DDW or cell culture medium (DMEM) were determined with DLS Particle Sizer (Brookhaven). For transmission electron microscopy (TEM) analysis, 20 μl of the biosynthesized AuNPs was dropped on copper grids layered with a fomvar-carbon film and air-dried for 30 min at room temperature. Finally, the image was taken on a field emission TEM (Jeol 2010 F, 80 keV). Fourier transform infrared spectroscopy (FTIR) analysis of leaf extract of *C. medica* and biosynthesized AuNPs were determined on a Perkin-Elmer Frontier instrument using a KBr sample. X-ray diffraction

(XRD) analysis was done on a Bruker D8 QUEST diffractometer system at λ of 1.54178 Å. All assays were done at room temperature and the samples were diluted with DDW.

2.4. Cell culture

HepG2 (human liver cancer cell line) and THLE3 (normal adult liver epithelial cells) were obtained from (ATCC, Shanghai, China) and cultured based on the previous report (Carlson et al., 2008) in minimum essential medium (MEM, Gibco, USA) and bronchial epithelial cell growth medium (BEBM Gibco, USA), respectively supplemented with essential materials (Carlson et al., 2008).

2.5. MTT assay

The effect of different concentrations of biosynthesized AuNPs (1, 10, 50, 100, and 200 µg/mL) on HepG2 and THLE3 cell viability was assessed by MTT assay. Briefly, 1×10^4 cells/100 µl/well of the cells suspended in cell culture media after 24 h were added by different concentrations of biosynthesized AuNPs and incubated for 24 h in a CO_2 incubator. Afterwards, the supernatant was replaced with 100 µl MTT solution (5 mg/mL in medium) and incubated for 4 h, followed by replacement of the culture media with DMSO (100 µl). The optical density of samples was then read at 540 nm using a Bio-Tek microplate reader.

2.6. Levels of malondialdehyde (MDA), superoxide dismutase (SOD) activity, and glutathione (GSH)

After treatment of HepG2 cells with IC_{50} concentration of biosynthesized AuNPs for 24 h, cells were washed, lysed with lysis buffer for 30 min, centrifuged (14000 rpm for 5 min, 4 °C), and protein concentration was determined in supernatant using BCA protein assay kit (Sigma-Aldrich, Shanghai, China). Afterwards, the levels of MDA production, GSH, and SOD activity were determined by Lipid Peroxidation (MDA) Assay Kit (233471, Abcam), GSH Assay Kit (703002, Cayman chemical), and SOD Activity Assay Kit (65354, Abcam) according to the manufacturer's protocols.

2.7. ROS assay

After treatment of the HepG2 cancer cells with IC_{50} concentration of biosynthesized AuNPs, the generation of intracellular ROS was determined using DCFH-DA probe on a microplate spectrofluorometer (GeminiXPS, USA) based on the method discussed previously (Carlson et al., 2008).

2.8. Quantitative real-time PCR (qPCR) analysis

Real-time PCR was done by use of the SYBR Green dye (Sigma-Aldrich, Shanghai, China) using the CFX96 real-time PCR detection system.

After treatment with AuNPs, total RNA was extracted by Trizole according to the manufacturer's instructions (GeneAll® RiboEx, Korea). The ratio of absorbance at 260/280 nm was read on a Nanodrop 1000 spectrophotometer (Thermo Fisher Scientific). Then, 2 µg of total RNA were converted to cDNA by Revert Aid First-strand cDNA synthesis Kit (Fermentas, Germany). cDNA was then applied for real-time quantitative RT-PCR. The reaction and fold change of mRNA expression were done based on the previous report (Mitupatum et al., 2016).

2.9. Western blot

The protein was extracted from HepG2 cells after 24 h incubation with IC_{50} concentration of biosynthesized AuNPs and quantified using BCA protein assay kit (Sigma-Aldrich, Shanghai, China). Then, a fixed amount of protein was loaded onto SDS-PAGE (10%) and run at 100 V for 70 min., followed by transferring to a polyvinylidene fluoride (PVDF) membrane for 60 min, blocking with dry milk (5%) and Tween-20 (0.1%) for 50 min at room temperature, incubation with primary antibodies (1:5,000; Santa Cruz Biotechnology, Inc.) overnight at 4 °C, and incubation with HRP-conjugated secondary antibodies (1:10,000; Santa Cruz Biotechnology, Inc.) for 60 min at room temperature. Finally, membranes were produced on an autoradiographic film.

2.10. Statistical analysis

The data were assessed by using one-way ANOVA and Tukey or Dunnett post hoc test, and outcomes were reported as average ± SD of three independent experiments. $P < 0.05$ was considered statistically significant.

3. Results and discussion

3.1. UV–visible study and total polyphenol assay

The UV–visible spectra of leaf extract of *C. medica* and biosynthesized AuNPs are depicted in Fig. 1, where the spectrum of

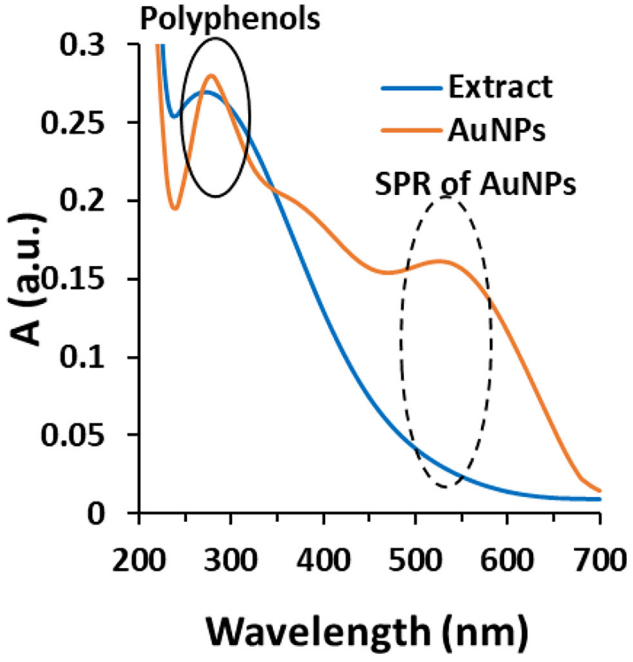

Fig. 1 UV–visible study of biosynthesized AuNPs using leaf extract of *Citrus medica*. The extract was used as the control.

extract show an absorbance with a λmax around 280 nm, indicating the presence of a high content of polyphenolic compounds (Ieri et al., 2021). Analyzing the level of polyphenolic compounds in leaf extract of *C. medica* is crucial because these bioactive agents are involved in the bio-reduction of Au ions to AuNPs. Once metallic NPs are synthesized, polyphenolic compounds along with some other bioactive compounds by attaching on the surface of NPs result in the stability of NPs.

The value of 327.23 ± 31.28 mg/g gallic acid and 48.94 ± 3.53 mg/g gallic acid determined from total polyphenols assay of leaf extract of *C. medica* alone and leaf extract of *C. medica* in the presence of $HAuCl_4$ revealed that the high polyphenolic content in leaf extract of *C. medica* is involved in the biosynthesis of AuNPs through the reducing the synthesis reaction and stabilizing the NPs (Karthick et al., 2012; Oueslati et al., 2020).

Fig. 1 demonstrates the characteristic absorption spectrum of biosynthesized AuNPs from leaf extract of *C. medica* in the region of 200–700 nm. SPR for biosynthesized AuNPs depicts a well characteristic band having an absorption with λmax of 550 nm. A similar spectrum has been reported in biosynthesis of AuNPs using extracts of *Ricinus communis* (Rahman et al., 2021); *Ganoderma applanatum* (Abdul-Hadi et al., 2020), and *Syzygium polyanthum* (Hasyim et al., 2020). Additionally, the AuNPs spectrum displays an absorption band around 280 nm, attributing to the presence of polyphenolic compounds of the extract as stabilizer agents of the AuNPs (Oueslati et al., 2020).

3.2. Hydrodynamic size and zeta potential of biosynthesized AuNPs

Hydrodynamic radius (Fig. 2a) and zeta potential (Fig. 2b) values of biosynthesized AuNPs at different conditions (DDW and DMEM) for a fixed concentration were determined (Fig. 2) and tabulated in Table 1. It was shown that biosynthesized AuNPs provided a negative value in DDW, indicating the potential electrostatic stability of NPs. However, zeta potential of biosynthesized AuNPs dispersed in DMEM was lower than that in DDW (Table 1).

This reduction in zeta potential value of biosynthesized AuNPs can be associated with the presence of cations and FBS in DMEM solution interacting with AuNPs surfaces which lead to a mitigation in electrostatic interactions and corresponding stability. Despite this significant reduction in zeta potential value, the zeta potential values of AuNPs in the range of −9-74 to −18.26 mV in both media, indicating the probable electrostatic stability of NPs (Mahmoud et al., 2020). Furthermore, Table 1 summarizes the hydrodynamic radii analyzed by DLS for biosynthesized AuNPs in DDW and DMEM at 37 °C. It was found that in DMEM medium, the hydrodynamic size of biosynthesized AuNPs was enhanced due to probable biomolecules adsorption on the NP surface (Mahmoud et al., 2020). This data could support the slightly smaller value on zeta potential for biosynthesized AuNPs dispersed in DMEM compared to that in DDW (Mahmoud et al., 2020).

Table 1 Hydrodynamic radius and zeta potential of biosynthesized AuNPs.

Medium	Hydrodynamic radius (nm)	Zeta potential (mV)
DDW (37 °C)	224	−18.26
DMEM (37 °C)	381	−9.74

3.3. Transmission electron microscopy (TEM) analysis

AuNPs TEM image is shown in Fig. 3 revealing the small diversity in the morphology of biosynthesized AuNPs. It has been reported that AuNPs shape is affected by the relationship between the initial concentration of metal ions and plant extract (Singh et al., 2018). In this case, as detected in Fig. 3, NPs had a size in the range of 20–50 nm. Some other plant-based extracts such as *Sphaeranthus indicus* (Balalakshmi et al., 2017); *Stemona tuberosa* (Bonigala et al., 2018), and *Pongamia pinnata* (Khatua et al., 2020) have also been used for the fabrication of AuNPs and it has been found that the size of synthesized NPs have been comparable to this study.

3.4. FTIR analysis

FTIR spectra, demonstrated in Fig. 4, attribute to leaf extract of *C. medica* and biosynthesized AuNPs. The broad band around 3350 cm^{-1} corresponds to phenolic OH which mainly

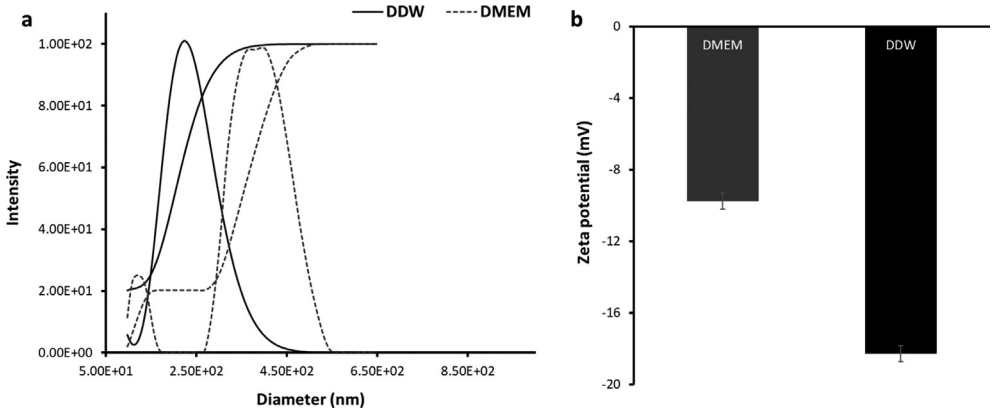

Fig. 2 DLS study of biosynthesized AuNPs using leaf extract of *Citrus medica* dissolved in DDW or DMEM. (a) diameter assay, (b) zeta potential assay.

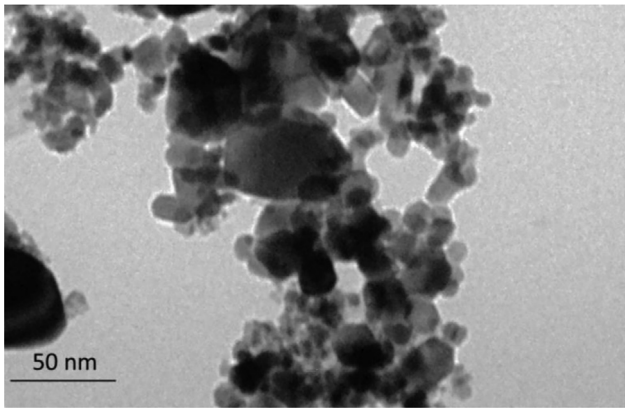

Fig. 3 TEM analysis of biosynthesized AuNPs using leaf extract of *Citrus medica*.

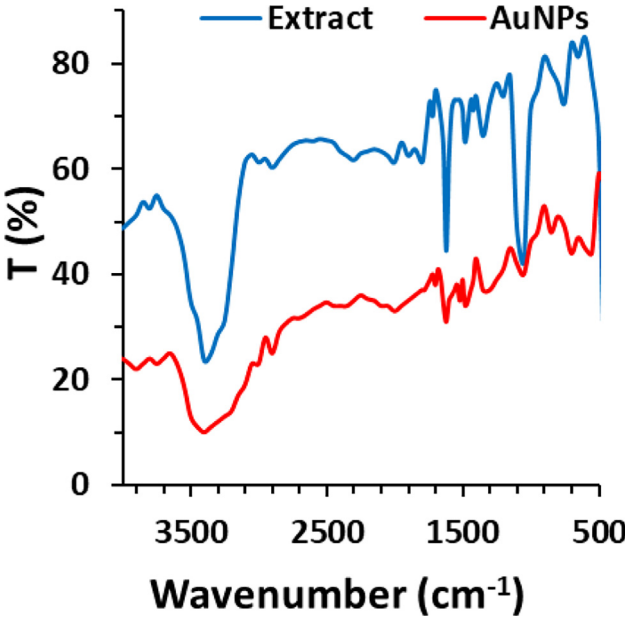

Fig. 4 FTIR study of biosynthesized AuNPs using leaf extract of *Citrus medica*. The extract was used as the control.

derive from tannins and flavonoids compounds. Peaks at 1569 cm^{-1} and 1729 cm^{-1} and region between 1000 and 1400 cm^{-1} correspond to N—H bending vibration, ketone acyclic stretch, and C—O stretch, respectively Also, bands in the range from 1500 to 500 cm^{-1} are associated with the presence of polyphenols as the most abundant bioactive metabolites in leaf extract of *C. medica*. The biosynthesized AuNPs display the similar characteristic bands in the region of polyphenols revealing that these NPs are stabilized by biomolecules of extract of *C. medica* (Karthick et al., 2012). We also detected an alteration in the width and intensity of band around 1348 cm^{-1} for biosynthesized AuNPs attributed to bond formation between biosynthesized AuNPs and C—H group of polyphenols; 1722 cm^{-1}, is shifted by conversion of polyphenolic into carboxylic groups upon synthesis of AuNPs (Ahmad et al., 2019; Karthick et al., 2012; Oueslatiet al., 2020).

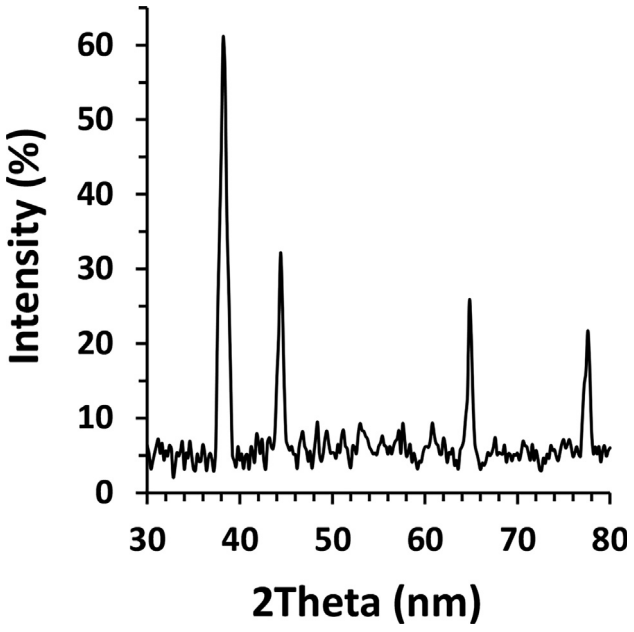

Fig. 5 XRD study of biosynthesized AuNPs using leaf extract of *Citrus medica*.

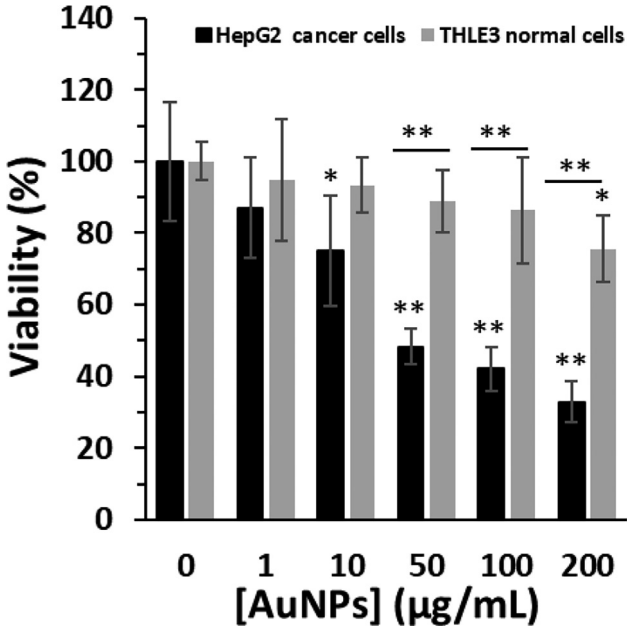

Fig. 6 The cytotoxic effects of biosynthesized AuNPs using leaf extract of *Citrus medica* on the viability of HepG2 (human liver cancer cell line) and THLE3 (normal adult liver epithelial cells) determined by MTT assay. The cells were incubated with biosynthesized AuNPs or leaf extract for 24 h. *P < 0.05, **P < 0.01 relative to control samples.

3.5. X-ray diffraction (XRD) analysis

Fig. 5 depicts the characteristic biosynthesized AuNPs XRD diffraction bands at 2θ, which centered at 38.21°, 44.39°, 65.01°, and 77.61° attributed to the planes (111), (200),

(220), and (311), respectively. These planes revealed the face-centered cubic Au (ICDD File No. 89-3722) (Rodríguez-León et al., 2019).

3.6. Cytotoxicity by MTT assay

To evaluate the anticancer effect of biosynthesized AuNPs, MTT assay was performed on HepG2 (human liver cancer cell line) and THLE3 (normal adult liver epithelial cells). Five concentrations (1, 10, 50, 100, and 200 μg/mL) and one time (24 h) for biosynthesized AuNPs were examined. In Fig. 6, it is realized that at 24 h for THLE3 normal cells, cell viability finally drops to 75.57 ± 3.27 % (*P < 0.05) at the presence of highest concentrations of AuNPs, *i,e*, 200 μg/mL However, for HepG2 cells, a more cytotoxic effect is obtained in cell viability; as the AuNPs concentrations above 10 μg/mL found to induce significant cytotoxic effects. In fact, for biosynthesized AuNPs, it is easy to find that concentration with the highest effect is 200 μg/mL, where the viability reduces almost 75.57 ± 3.27 % and 32.89 ± 5.87 % for THLE3 normal cells and HepG2 cancer cells, respectively, as compared to the control after 24 h (Fig. 6). Therefore, it was observed that biosynthesized AuNPs were significantly more toxic to HepG2 cancer cells relative to THLE3, with up to 2.2-fold higher cell death (**P < 0.01) in the cancer cells at concentration of 200 μg/mL.

For THLE3 normal cells, a significant toxic effect is observed only at 200 μg/mL biosynthesized AuNPs (*P < 0.05), while lower concentrations show no significant difference, compared to control sample (Fig. 6). However, for HepG2 cancer cells, a significant cytotoxicity is detected at 10 μg/mL biosynthesized AuNPs, and the inhibition of cell growth rate was further increased as the concentrations of AuNPs were increased after 24 h. It was then determined that the IC_{50} concentration of biosynthesized AuNPs against HepG2 cells was about 44.87 μg/mL. Therefore, for further experiments, the cells were incubated with 45 μg/mL of AuNPs.

It has been also reported that IC_{50} of biosynthesized AuNPs from licorice root (Al-Radadi, 2021) and *Cordyceps militaris* (Ji et al., 2019) were 23 μg/mL and 10 μg/mL, respectively for HepG-2 cells.

3.7. ROS assays

To investigate the generation of intracellular ROS in HepG2 cells after exposure with IC_{50} concentration of biosynthesized

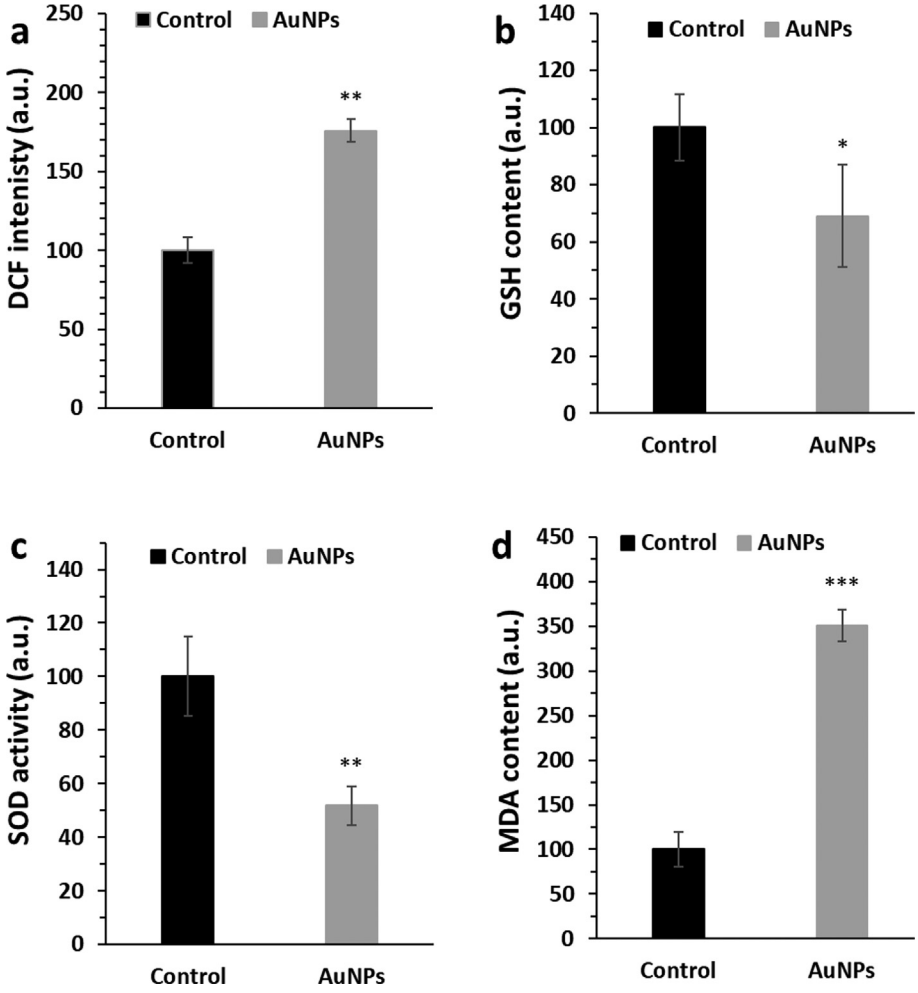

Fig. 7 The effects of biosynthesized AuNPs (45 μg/mL) using leaf extract of *Citrus medica* on induction of oxidative stress through analysis of (a) ROS, (b) GSH content, (c) SOD activity, (d) MDA level in HepG2 (human liver cancer cell line) cells. The HepG2 cells were incubated with biosynthesized AuNPs for 24 h. *P < 0.05, **P < 0.01 relative to control samples.

AuNPs (45 μg/mL), we assessed the conversion of non-fluorescence H_2-DCFDA probe into fluorescence dichlorodihydrofluorescein (DCF) probe. Outcomes showed that HepG2 cells exposed to biosynthesized AuNPs (45 μg/mL) significantly increased the generation of ROS, revealed by a significant increase in the level of DCF fluorescence intensity (Fig. 7a).

It was also found that biosynthesized AuNPs (45 μg/mL) significantly dropped the levels of GSH content (Fig. 7b) and SOD activity (Fig. 7c) and increased the level of MDA content (Fig. 7d) as a marker of lipid peroxidation.

It has been also reported that plant-based AuNPs induce anticancer activity through a significant increase in the generation of intracellular ROS and stimulation of oxidative stress (Khatua et al., 2020; Wang et al., 2019).

3.8. Apoptosis assays

It was seen that expression levels of apoptotic genes such as *Bax* and *Caspase-3* increased, whereas the expression level of antiapoptotic mRNA (*Bcl-2*) was decreased after exposure of HepG2 cells with 45 μg/mL of AuNPs for 24 h (Fig. 8), which is in consistent with previous studies (Khatua et al., 2020; Ramalingam et al., 2016), revealing the induction of apoptosis by AuNPs.

In fact, this data further verifies that the selective anticancer effects of biosynthesized AuNPs are mediated by apoptosis induction in HepG2-cells. It has been also reported that biosynthesized AuNPs using *Cardiospermum halicacabum* (Li et al., 2019), *Curcuma wenyujin* (Liu et al., 2019); and *Catharanthus roseus* (Ke et al., 2019) extracts can induce anticancer effects through Bax, Bcl, and Caspase-mediated apoptotic pathway.

3.9. Signaling pathway assay

It was seen that biosynthesized AuNPs triggered oxidative stress and apoptosis in HepG2 cancer cells. Oxidative stress usually stimulates the phosphorylation of p38 MAP kinase and results in the induction of apoptosis in several types of cancers (Yan et al., 2012). In the present study, we also found significant increase in the expression of phosphorylated p38 at protein level in HepG2 cells after exposure to biosynthesized

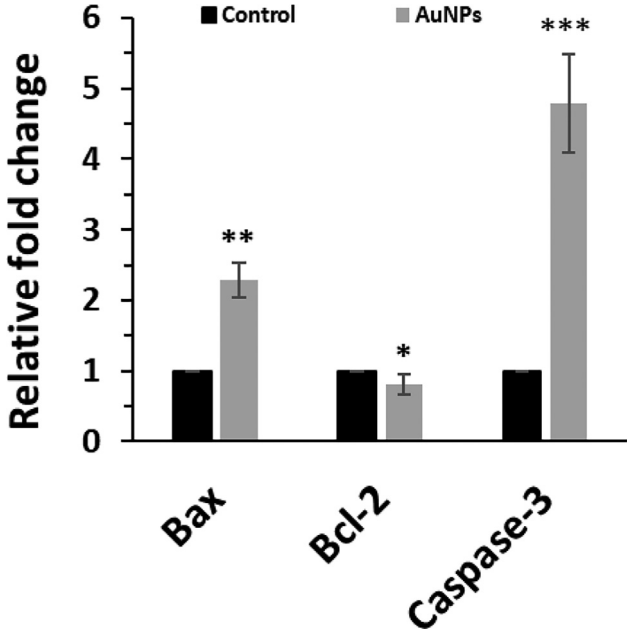

Fig. 8 The effects of biosynthesized AuNPs (45 μg/mL) using leaf extract of *Citrus medica* on expression of *Bax, Bcl-2,* and *Capsase-3* determined by qPCR assay in HepG2 (human liver cancer cell line) cells. The HepG2 cells were incubated with biosynthesized AuNPs for 24 h. *P < 0.05, **P < 0.01, ***P < 0.001 relative to control samples.

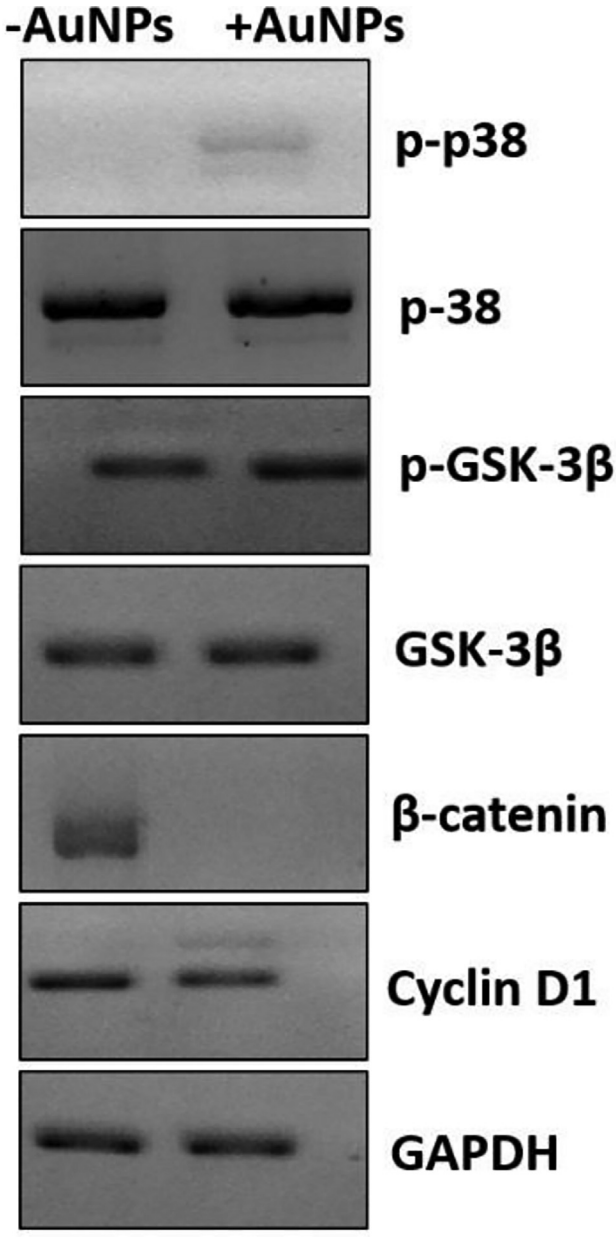

Fig. 9 The effects of biosynthesized AuNPs (45 μg/mL) using leaf extract of *Citrus medica* on regulation of Wnt signaling pathways determined by western blot analysis in HepG2 (human liver cancer cell line) cells. The HepG2 cells were incubated with biosynthesized AuNPs for 24 h.

AuNPs (45 μg/mL) (Fig. 9), which caused the increase in the expression level of phosphorylated GSK-3β (p-GSK-3β-ser-9) as the inactivated form of GSK-3β. Furthermore, phosphorylation of GSK-3β can reduce the expression level of β-catenin and block the expression of target oncogenes like Cyclin D1 (Viganotti et al., 2010). The GSK-3β, β-catenin, and Cyclin D1 are known as the main proteins which play a key role in the regulation of the Wnt/β-catenin signaling pathway (Shi et al., 2016). We observed that biosynthesized AuNPs increased the expression of phosphorylated GSK-3β at protein level known as the inactivated form of GSK-3β to drop the expressions of β-catenin and Cyclin-D1 at protein level as the targeted markers (Fig. 9). Therefore, this data indicated that AuNPs induced anticancer effects against HepG2 cells through ROS-mediated apoptosis via regulation of the Wnt/β-catenin signaling pathway.

4. Conclusions

In conclusion, we biosynthesized a bioinspired plant-based AuNPs with the traditional medicinal herb C. medica and explored their potential selective anticancer affects against HepG2 cancer cells induced by ROS-mediated apoptosis through Wnt/β-catenin signaling pathway. In summary, our outcomes indicated that biosynthesized AuNPs from leaf extract of *C. medica* can be considered as a potent anticancer drug against HCC. However, the yield of AuNPs, stability as well as dissolution of AuNPs into Au ions can considerably influence the stability and anticancer effects of AuNPs, which needs further examinations in the future studies. Also, the anticancer effects of AuNPs should be further verified *in vivo* in the future studies.

Declaration of Competing Interest

The authors declare that they have no known competing financial interests or personal relationships that could have appeared to influence the work reported in this paper.

Acknowledgment

The authors would like to thank Le Lu, the Xi'an Jiaotong University, for help in western blot assay.

References

Abdul-Hadi, S.Y., Owaid, M.N., Rabeea, M.A., Aziz, A.A., Jameel, M.S., 2020. Rapid mycosynthesis and characterization of phenols-capped crystal gold nanoparticles from Ganoderma applanatum, Ganodermataceae. Biocatal. Agric. Biotechnol. 1 (27), 101683.

Ahmad, T., Bustam, M.A., Irfan, M., Moniruzzaman, M., Asghar, H. M., Bhattacharjee, S., 2019. Mechanistic investigation of phytochemicals involved in green synthesis of gold nanoparticles using aqueous Elaeis guineensis leaves extract: Role of phenolic compounds and flavonoids. Biotechnol. Appl. Biochem. 66 (4), 698–708.

Al-Radadi, N.S., 2021. Facile one-step green synthesis of gold nanoparticles (AuNp) using licorice root extract: Antimicrobial and anticancer study against HepG2 cell line. Arab. J. Chem. 14 (2), 102956.

Balalakshmi, C., Gopinath, K., Govindarajan, M., Lokesh, R., Arumugam, A., Alharbi, N.S., Kadaikunnan, S., Khaled, J.M., Benelli, G., 2017. Green synthesis of gold nanoparticles using a cheap Sphaeranthus indicus extract: Impact on plant cells and the aquatic crustacean Artemia nauplii. J. Photochem. Photobiol. B Biol. 1 (173), 598–605.

Bonigala, B., Kasukurthi, B., Konduri, V.V., Mangamuri, U.K., Gorrepati, R., Poda, S., 2018. Green synthesis of silver and gold nanoparticles using Stemona tuberosa Lour and screening for their catalytic activity in the degradation of toxic chemicals. Environ. Sci. Pollut. Res. 25 (32), 32540–32548.

Carlson, C., Hussain, S.M., Schrand, A.M., Braydich-Stolle, K.L., Hess, K.L., Jones, R.L., Schlager, J.J., 2008. Unique cellular interaction of silver nanoparticles: Size-dependent generation of reactive oxygen species. J. Phys. Chem. B 112 (43), 13608–13619.

Chandhirasekar, K., Thendralmanikandan, A., Thangavelu, P., Nguyen, B.S., Nguyen, T.A., Sivashanmugan, K., Nareshkumar, A., Nguyen, V.H., 2021. Plant-extract-assisted green synthesis and its larvicidal activities of silver nanoparticles using leaf extract of Citrus medica, Tagetes lemmonii, and Tarenna asiatica. Mater. Lett. 15 (287), 129265.

Chhikara, N., Kour, R., Jaglan, S., Gupta, P., Gat, Y., Panghal, A., 2018. Citrus medica: Nutritional, phytochemical composition and health benefits–a review. Food Funct. 9 (4), 1978–1992.

Conde-Hernández, L.A., Guerrero-Beltrán, J.Á., 2014. Total phenolics and antioxidant activity of Piper auritum and Porophyllum ruderale. Food Chem. 142, 455–460.

de Camargo, A.C., Regitano-d'Arce, M.A.B., Biasoto, A.C.T., Shahidi, F., 2014. Low molecular weight phenolics of grape juice and winemaking byproducts: Antioxidant activities and inhibition of oxidation of human low-density lipoprotein cholesterol and DNA strand breakage. J. Agric. Food Chem. 62 (50), 12159–12171.

Devarakonda, S.B., Myers, M.R., Lanier, M., Dumoulin, C., Banerjee, R.K., 2017. Assessment of gold nanoparticle-mediated-enhanced hyperthermia using MR-guided high-intensity focused ultrasound ablation procedure. Nano Lett. 17 (4), 2532–2538.

Elizabeth, M.K., Devi, R.U., Raja, K.P., Krishna, K.B., 2022. Synthesis of phyto based metal nanoparticles: A green approach. J. Pharmaceut. Res. Int. 34 (25A), 20–32.

Falahati, M., Attar, F., Sharifi, M., Saboury, A.A., Salihi, A., Aziz, F. M., Kostova, I., Burda, C., Priecel, P., Lopez-Sanchez, J.A., Laurent, S., 2020. Gold nanomaterials as key suppliers in biological and chemical sensing, catalysis, and medicine. Biochim. Biophys. Acta (BBA)-General Subjects. 1864 (1), 129435.

Fratianni, F., Cozzolino, A., De Feo, V., Coppola, R., Ombra, M.N., Nazzaro, F., 2019. Polyphenols, antibacterial, and biofilm inhibitory activities of peel and pulp of Citrus medica L., Citrus bergamia, and Citrus medica cv. Salò Cultivated in Southern Italy. Molecules 24 (24), 4577.

Hasyim, M.F., 2020. A Synthesis and Characterization of Gold Nanoparticles Using The Bioreductor Bay Leaf (Syzygium polyanthum). Jurnal Akta Kimia Indonesia (Indonesia Chimica Acta). 31, 79–84.

Ieri, F., Campo, M., Cassiani, C., Urciuoli, S., Jurkhadze, K., Romani, A., 2021. Analysis of aroma and polyphenolic compounds in Saperavi red wine vinified in Qvevri. Food Sci. Nutr..

Ji, Y., Cao, Y., Song, Y., 2019. Green synthesis of gold nanoparticles using a Cordyceps militaris extract and their antiproliferative effect in liver cancer cells (HepG2). Artif. Cells Nanomed. Biotechnol. 47 (1), 2737–2745.

Karthick, V., Ganesh Kumar, V., Maiyalagan, T., Deepa, R., Govindaraju, K., Rajeswari, A., Stalin, D.T., 2012. Green synthesis of well dispersed nanoparticles using leaf extract of medicinally useful Adhatoda vasica nees. Micro Nanosyst. 4 (3), 192–198.

Ke, Y., Al Aboody, M.S., Alturaiki, W., Alsagaby, S.A., Alfaiz, F.A., Veeraraghavan, V.P., Mickymaray, S., 2019. Photosynthesized gold nanoparticles from Catharanthus roseus induces caspase-mediated apoptosis in cervical cancer cells (HeLa). Artif. Cells Nanomed. Biotechnol. 47 (1), 1938–1946.

Kennedy, L.C., Bickford, L.R., Lewinski, N.A., Coughlin, A.J., Hu, Y., Day, E.S., West, J.L., Drezek, R.A., 2011. A new era for cancer treatment: Gold-nanoparticle-mediated thermal therapies. Small 7 (2), 169–183.

Khalaf, A.M., Fuentes, D., Morshid, A.I., Burke, M.R., Kaseb, A.O., Hassan, M., Hazle, J.D., Elsayes, K.M., 2018. Role of Wnt/β-catenin signaling in hepatocellular carcinoma, pathogenesis, and clinical significance. J. Hepatocellular Carcinoma. 5, 61.

Khatua, A., Prasad, A., Priyadarshini, E., Patel, A.K., Naik, A., Saravanan, M., Barabadi, H., Paul, B., Paulraj, R., Meena, R., 2020. Emerging antineoplastic plant-based gold nanoparticle synthesis: A mechanistic exploration of their anticancer activity toward cervical cancer cells. J. Clust. Sci. 31 (6), 1329–1340.

Khatua, A., Priyadarshini, E., Rajamani, P., Patel, A., Kumar, J., Naik, A., Saravanan, M., Barabadi, H., Prasad, A., Paul, B., Meena, R., 2020. Phytosynthesis, characterization and fungicidal potential of emerging gold nanoparticles using Pongamia pinnata leave extract: A novel approach in nanoparticle synthesis. J. Clust. Sci. 31 (1), 125–131.

Li, C., Wang, Y., Zhang, H., Li, M., Zhu, Z., Xue, Y., 2019. An investigation on the cytotoxicity and caspase-mediated apoptotic effect of biologically synthesized gold nanoparticles using Cardiospermum halicacabum on AGS gastric carcinoma cells. Int. J. Nanomed. 14, 951.

Liu, R., Pei, Q., Shou, T., Zhang, W., Hu, J., Li, W., 2019. Apoptotic effect of green synthesized gold nanoparticles from Curcuma wenyujin extract against human renal cell carcinoma A498 cells. Int. J. Nanomed. 14, 4091.

Lou, Z., Chen, J., Yu, F., Wang, H., Kou, X., Ma, C., Zhu, S., 2017. The antioxidant, antibacterial, antibiofilm activity of essential oil from Citrus medica L. var. sarcodactylis and its nanoemulsion. LWT. 1 (80), 371–377.

Mahmoud, N.N., Abu-Dahab, R., Abdallah, M., Al-Dabash, S., Abuarqoub, D., Albasha, A., Khalil, E.A., 2020. Interaction of gold nanorods with cell culture media: Colloidal stability, cytotoxicity and cellular death modality. J. Drug Delivery Sci. Technol. 1 (60), 101965.

McGlynn, K.A., Petrick, J.L., El-Serag, H.B., 2021. Epidemiology of hepatocellular carcinoma. Hepatology 73, 4–13.

Menichini, F., Loizzo, M.R., Bonesi, M., Conforti, F., De Luca, D., Statti, G.A., de Cindio, B., Menichini, F., Tundis, R., 2011. Phytochemical profile, antioxidant, anti-inflammatory and hypoglycemic potential of hydroalcoholic extracts from Citrus medica L. cv Diamante flowers, leaves and fruits at two maturity stages. Food Chem. Toxicol. 49 (7), 1549–1555.

Mitropoulou, G., Fitsiou, E., Spyridopoulou, K., Tiptiri-Kourpeti, A., Bardouki, H., Vamvakias, M., Panas, P., Chlichlia, K., Pappa, A., Kourkoutas, Y., 2017. Citrus medica essential oil exhibits significant antimicrobial and antiproliferative activity. LWT. 1 (84), 344–352.

Mitupatum, T., Aree, K., Kittisenachai, S., Roytrakul, S., Puthong, S., Kangsadalampai, S., Rojpibulstit, P., 2016. mRNA expression of Bax, Bcl-2, p53, cathepsin B, caspase-3 and caspase-9 in the HepG2 cell line following induction by a novel monoclonal Ab Hep88 mAb: Cross-talk for paraptosis and apoptosis. Asian Pac. J. Cancer Prev. 17 (2), 703–712.

Nair, A., Kurup Sr, R., Nair, A.S., Baby, S., 2018. Citrus peels prevent cancer. Phytomedicine 15 (50), 231–237.

Oueslati, M.H., Ben Tahar, L., Harrath, A.H., 2020. Synthesis of ultra-small gold nanoparticles by polyphenol extracted from Salvia officinalis and efficiency for catalytic reduction of p-nitrophenol and methylene blue. Green Chem. Lett. Rev. 13 (1), 18–26.

Rahman, T.U., Khan, H., Liaqat, W., Zeb, M.A., 2021. Phytochemical screening, green synthesis of gold nanoparticles, and antibacterial activity using seeds extract of Ricinus communis L. Microsc. Res. Tech. 1 (1), 1–10.

Ramalingam, V., Revathidevi, S., Shanmuganayagam, T., Muthulakshmi, L., Rajaram, R., 2016. Biogenic gold nanoparticles induce cell cycle arrest through oxidative stress and sensitize mitochondrial membranes in A549 lung cancer cells. RSC Adv. 6 (25), 20598–20608.

Rodríguez-León, E., Rodríguez-Vázquez, B.E., Martínez-Higuera, A., Rodríguez-Beas, C., Larios-Rodríguez, E., Navarro, R.E., López-Esparza, R., Iñiguez-Palomares, R.A., 2019. Synthesis of gold nanoparticles using Mimosa tenuiflora extract, assessments of cytotoxicity, cellular uptake, and catalysis. Nanoscale Res. Lett. 14 (1), 1–6.

Sharifi, M., Attar, F., Saboury, A.A., Akhtari, K., Hooshmand, N., Hasan, A., El-Sayed, M.A., Falahati, M., 2019. Plasmonic gold nanoparticles: Optical manipulation, imaging, drug delivery and therapy. J. Control. Release 1 (311), 170–189.

Shi, Q., Shi, X., Zuo, G., Xiong, W., Li, H., Guo, P., Wang, F., Chen, Y., Li, J., Chen, D.L., 2016. Anticancer effect of 20 (S)-ginsenoside Rh2 on HepG2 liver carcinoma cells: Activating GSK-3β and degrading β-catenin. Oncol. Rep. 36 (4), 2059–2070.

Siddique, M., Khan, N.M., Saeed, M., Ali, S., Shah, Z., 2021. Green synthesis of cobalt oxide nanoparticles using Citrus medica leaves extract: Characterization and photo-catalytic activity. Z. Phys. Chem. 235 (6), 663–681.

Singh, H., Du, J., Singh, P., Yi, T.H., 2018. Ecofriendly synthesis of silver and gold nanoparticles by Euphrasia officinalis leaf extract and its biomedical applications. Artif. Cells Nanomed. Biotechnol. 46 (6), 1163–1170.

Taghvaeefard, N., Ghani, A., Hosseinifarahi, M., 2021. Comparative study of phytochemical profile and antioxidant activity of flavedo from two Iranian citron fruit (Citrus medica L.). J. Food Meas. Charact. 15 (3), 2821–2830.

Viganotti, M., Antoccia, A., Magrelli, A., Salvatore, M., Azzalin, G., Tosto, F., Lorenzetti, S., Maranghi, F., Mantovani, A., Macino, G., Tanzarella, C., 2010. Characterization of HuH6, Hep3B, HepG2 and HLE liver cancer cell lines by WNT/β-catenin pathway, microRNA expression and protein expression profile. Cell. Mol. Biol. 56 (3), 1299–11297.

Vijayaraghavan, K., Ashokkumar, T., 2017. Plant-mediated biosynthesis of metallic nanoparticles: A review of literature, factors affecting synthesis, characterization techniques and applications. J. Environ. Chem. Eng. 5 (5), 4866–4883.

Wang, L., Xu, J., Yan, Y., Liu, H., Karunakaran, T., Li, F., 2019. Green synthesis of gold nanoparticles from Scutellaria barbata and its anticancer activity in pancreatic cancer cell (PANC-1). Artif. Cells Nanomed. Biotechnol. 47 (1), 1617–1627.

Yan, F., Wang, M., Li, J., Cheng, H., Su, J., Wang, X., Wu, H., Xia, L., Li, X., Chang, H.C., Li, Q., 2012. Gambogenic acid induced mitochondrial-dependent apoptosis and referred to phospho-Erk1/2 and phospho-p38 MAPK in human hepatoma HepG2 cells. Environ. Toxicol. Pharmacol. 33 (2), 181–190.